Effect of backbond oxidation on silicon nanocrystallites

L. E. Ramos, J. Furthmüller, and F. Bechstedt
Institut für Festkörpertheorie und Theoretische Optik, Friedrich-Schiller-Universität Jena, 07743 Jena, Germany
(Received 26 March 2004; published 29 July 2004)

We employ density functional calculations to study properties of Si nanocrystals after backbond oxidation in comparison to the ones passivated with hydrogen or hydroxyl. Structural parameters, pair excitation energies, quasiparticle gaps, and electrostatic potentials vary significantly in dependence on degree of oxidation and surface passivation. The variations are discussed within a quantum confinement picture. Blueshifts and redshifts observed in photoluminescence are related to the size of the Si nanocrystallite cores and the oxygen incorporation via passivation with group OH or oxidation.

DOI: 10.1103/PhysRevB.70.033311 PACS number(s): 73.22.−f, 78.67.Bf, 81.05.Kf

The investigation of silicon quantum structures is a very active field of research, due to the fundamental physical properties and promising applications in advanced optoelectronic and electronic devices.[1,2] Silicon-based nanocrystalline materials such as porous silicon (PSi) or silicon nanocrystals (NC's) exhibit an intense room-temperature photoluminescence (PL) in the visible spectral region,[3,4] whose mechanism is still under debate.[4,5] The most accepted models to explain the PL in nanosized materials are related to quantum confinement effects. Quantum confinement increases the radiative recombination and the optical gap of the NC's, thereby shifting the PL peaks in the visible spectral range.[4,6,7] However, numerous other mechanisms have been proposed to explain the PL, including surface/interface states, specific chemical compounds (e.g., siloxenes) or even defects in the host material (see discussion in Refs. 4 and 5).

The role of oxygen in the energetical position and efficiency of the PL has been demostrated for oxidized Si NC's and NC's embedded in certain SiO_2 matrices.[4,8–11] There are contradictory experimental results concerning the shift of the PL peak due to oxidation. While the PL blueshift from Si NCs embedded in SiO_2 matrices[10] and from the oxidation of porous Si (Ref. 11) seems to support the quantum confinement model, there is evidence that a PL redshift is caused by defect states.[4] Theoretical studies are usually limited to the effect of isolated O atoms at the NC surface.[12–15] Only in one case a complete OH surface termination has been related to the drastic gap shrinkage and reduction of the PL intensity.[8]

In this paper we study the variation of properties in nanometer-sized Si dots with backbond oxidation in comparison to those for H and OH passivations. To this end, we carry out first-principles calculations to derive optimized structures of the Si nanocrystallites, electronic structures, and optical absorption spectra. The calculations are based on the density-functional theory (DFT) within the local-density approximation (LDA).[16] The exchange-correlation contribution to the electron-electron interaction is described by the paramtrization of Perdew and Zunger. The electron-ion interaction is modeled by non-normconserving pseudopotentials which allow one to restrict the plane-wave cutoff to 22 Ry. This method is combined with the projector-augmented wave (PAW) method to construct the all-electron wave functions and calculate the optical matrix elements.[17] Bulk computations within the DFT-LDA yield cubic lattice constants of $a=5.404$ *Å* (Si) and $a=7.391$ *Å* (SiO_2, ideal β-cristobalite) or fundamental energy gaps of $E_{\mathrm{gap}}=0.44$ eV (Si) and $E_{\mathrm{gap}}=5.48$ eV (SiO_2).

Apart from the Stokes shift, the energetical PL peak position and the onset of the optical absorption are determined by the lowest electron-hole pair energy E_{pair}. For confined systems with free-exciton radii larger than the system extent such an energy can be calculated by a generalization of the delta-self-consistent-field (ΔSCF) method as differences of DFT-LDA total energies $E_{\mathrm{pair}}=E(N,e+h)-E(N)$, with the ground-state energy $E(N)$ of the considered N-electron system.[18] The total energy $E(N,e+h)$ of the system excited by an electron-hole pair is calculated with the constraint that the highest occupied molecular orbital (HOMO) state of the ground-state system contains a hole, placing the corresponding remaining electron automatically in the lowest unoccupied molecular orbital (LUMO) state of the ground-state system. $E(N,e+h)$ accounts for two effects of the electron-electron interaction after excitation. The interaction of the excited electron (hole) yields a quasiparticle (QP), whose energy is renormalized by self-energy effects and therefore shifted to higher (lower) energy. In addition, there is an attractive screened Coulomb interaction of the excited quasielectron and quasihole resulting in excitonic effects. According to the ΔSCF method, the quasiparticle gap without excitonic effects is defined by means of the total energies of the systems with $N+1$, N, and $N-1$ electrons, i.e., $E_{\mathrm{gap}}^{\mathrm{QP}}=E(N+1)+E(N-1)-2\,E(N)$.

Simple cubic (sc) supercells are used to model the NC's surrounded by vacuum. The symmetry of the NCs is constrained to T_d by starting from one central Si atom and adding its nearest neighbors, thereby assuming fourfold tetrahedral coordination. This procedure is repeated atomic shell by atomic shell up to the outermost Si shell, where the resulting dangling bonds are saturated by hydrogen atoms. The assumption of a diamondlike crystal structure is in accordance with recent measurements by high-resolution transmission electron microscopy (HRTEM).[19] The starting structures of NCs containing oxygen are obtained by introducing oxygen atoms in between the Si-Si bulk bonds at the outermost NC shells (backbond oxidation) or by replacing the H atoms at the surface termination by hydroxyl (OH) groups (passiva-

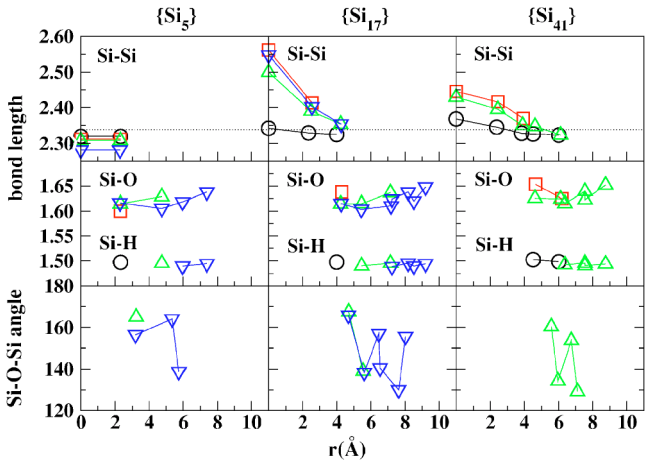

FIG. 1. (Color online) Average bond lengths (in *Å*) and Si-O -Si angles (in degrees) versus distance from center of the NCs for Si cores with varying size. The different oxidation stages are indicated by circles (H passivation), squares (OH passivation), up triangles (one oxide shell), and down triangles (two oxide shells). The dotted lines indicate the bulk Si bond length.

tion with OH). Models with backbond oxidation without destroying the Si-H bonds are supported by high-resolution electron energy loss spectroscopy (HREELS) (Ref. 20) and infrared (IR) absorption measurements.[21] We study Si NCs with cores containing 5, 17, and 41 Si atoms and up to two oxide shells. A vacuum region of at least 1 nm separates every NC from its supercell images, minimizing the NC-NC interaction. The large forces and stresses caused by the Si -O bond lengths of about 1.17 *Å* decrease after ionic relaxation, when the bond lengths are about 1.60 *Å*, i.e., the typical values of SiO_2 polymorphs. Due to the symmetry constraint of the ionic relaxation and initial Si-O bond lengths the minimization of the total energy is difficult and time consuming.

Results of structural optimization for Si NC's with the same Si core are shown in Fig. 1. The bond lengths of each atom were calculated and averaged shell by shell and plotted versus the distance from the atom to the center of the NC. As a result of the minimization of the total energy, the Si-Si bond lengths deviate from the bulk value differently in the core and close to the surface of the NC's. The molecular character of the NC's with the smallest core gives rise to Si -Si lengths slightly shortened with respect to the bulk value. On the contrary, the largest cores $\{Si_{17}\}$ and $\{Si_{41}\}$ exhibit an expansion of the Si-Si bonds in the core with a stronger effect at the center.[22] Oxidation of the nanocrystallites increases this effect, but for two oxide shells a saturation of the bond lengths occurs. The Si-O bonds lengths increase slightly close to the outermost shells of the NC. There is practically no variation of the Si-H bond lengths versus the NC radii. Qualitatively similar effects as shown in Fig. 1 have been found experimentally for oxidized Si NC's.[23,24] For small sizes the NC's are indeed expanded, whereas large particles with diameters larger than 3.5 nm exhibit a contraction of the lattice planes. The Si-O-Si angles are smaller than in the initial configuration (180°) and decrease with respect to the crystallite radius. The fact that the Si-O-Si angle decreases when an additional oxide shell is present indicates that the oxidation of the nanoparticle can be a self-limiting process and the limitation is related to the interface stress.[25]

TABLE I. Fundamental DFT-LDA gap E_{gap}, pair excitation energy E_{pair}, and quasiparticle gap E_{gap}^{QP}. The energies are given in eV and the number of atoms in the NC core is indicated in braces.

	E_{gap}	E_{pair}	E_{gap}^{QP}
$\{Si_5\}$-H_{12}	5.64	5.72	6.77
$\{Si_5\}$-$(OH)_{12}$	4.12	4.44	4.91
$\{Si_5\}$-$O_{12}Si_{12}H_{36}$	4.89	5.10	5.69
$\{Si_5\}$-$O_{48}Si_{36}H_{60}$	5.13	5.19	5.55
$\{Si_{17}\}$-H_{36}	4.17	4.20	5.08
$\{Si_{17}\}$-$(OH)_{36}$	2.99	3.14	4.05
$\{Si_{17}\}$-$O_{36}Si_{24}H_{60}$	3.39	3.44	4.32
$\{Si_{17}\}$-$O_{96}Si_{66}H_{108}$	3.25	3.31	3.96
$\{Si_{41}\}$-H_{60}	3.22	3.25	3.81
$\{Si_{41}\}$-$(OH)_{60}$	1.89	1.93	2.48
$\{Si_{41}\}$-$O_{60}Si_{42}H_{108}$	2.33	2.38	2.91

The influence of the oxidation on the electronic structure and hence the quantum confinement is presented in Table I and Fig. 2. The HOMO-LUMO gaps E_{gap}, the QP gaps E_{gap}^{QP}, and the pair excitation energies E_{pair} in Table I clearly demonstrate the quantum size effect versus the diameter of the Si cores. The values of the pair excitation energy and the DFT-LDA gap of the NCs are close to each other, indicating a cancellation of QP gap opening and Coulomb attraction of electrons and holes.[18] A comparison of the pair excitation energies with QP gaps gives an electron-hole attraction of 0.5–1.0 eV for the smallest NC's studied. The effect of the backbond oxidation is obvious by comparing the gaps of the crystallites $\{Si_{41}\}$-H_{60}, $\{Si_{17}\}$-$O_{36}Si_{24}H_{60}$, and $\{Si_5\}$ -$O_{48}Si_{36}H_{60}$, or the crystallites $\{Si_{17}\}$-H_{36} and $\{Si_5\}$ -$O_{12}Si_{12}H_{36}$. As a result of the oxidation, the gap is increased in dependence on the core size. This result is consistent with the experimental observation of a blueshift after the oxida-

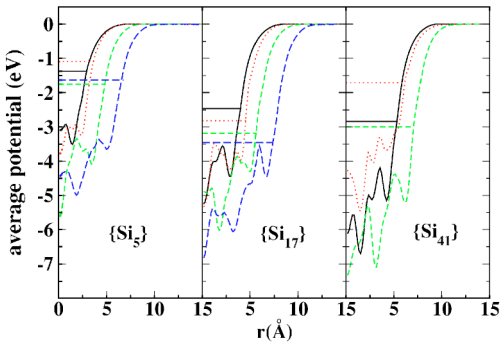

FIG. 2. (Color online) Average electrostatic potential along the ⟨001⟩ direction versus distance from the center of the NC. The positions of the LUMO states are indicated by horizontal lines. The curves are aligned with respect to the vacuum level (zero energy). Solid lines: hydrogenated NC's, dotted lines: OH termination, short-dashed lines: one oxide shell, and long-dashed lines: two oxide shells.

tion of NC's.[10,11] The size of the Si core seems to be the dominant factor for the magnitude of the gap and hence for the position of the PL peak. For the same NC core, however, an additional oxide shell reduces significantly the gap with respect to the NC passivated with H. There is a saturation of the gap when one compares the crystallites with one and two oxide shells, for instance, the NC's $\{Si_{17}\}$-$O_{36}Si_{24}H_{60}$ and $\{Si_{17}\}$-$O_{96}Si_{66}H_{108}$. On the other hand, the incorporation of oxygen via passivation with OH group implies no significant changes in the size of the Si core and a HOMO-LUMO gap much narrower than the one for the NC passivated with H and with one oxide shell. This tendency has been already observed for the adsorption of isolated O atoms and OH groups.[12–15] The inspection of the spatial distribution of HOMO and LUMO states shows that the pronounced gap shrinkage in the case of a complete passivation with OH is related to the delocalization of the LUMO state, the latter induced by the oxygen atoms in the outermost shells.

The influence of oxidation on the pair excitation energies may be explained by the variations of the electrostatic potential from the NC center into the vacuum region as shown in Fig. 2. Apart from oscillations due to the shell structure of the oxidized and hydrogenated NC's, the curves in Fig. 2 are similar to the spatial variation of the electron potential energy in a three-dimensional quasispherical quantum well. As expected, the width of the potential well for the NC's passivated with H and with OH is smaller than for the ones after backbond oxidation. As in a three-dimensional quantum well, the position of the LUMO state with respect to the vacuum level depends mainly on the effective size of the NC, i.e., the width of the potential well. The abrupt variation of the energetical position of the LUMO with the Si core size in the presence of an OH termination is a consequence of the different electrostatic interactions due to the number of dangling bonds at the surface facets saturated by -OH. In general, backbond oxidation increases both electron affinity and depth of the electron potential of the NC. This is not only consistent with the gap shrinkage (see Table I), but also with the localization of the single-particle wave functions. The presence of oxygen in the outermost shells delocalizes the LUMO state, while the HOMO state remains mainly localized at the center of the crystallite, as shown in Fig. 3 for $\{Si_{17}\}$ cores passivated with H and covered with an oxide shell. In all studied cases either the overlap between HOMO and LUMO wave functions is small or the oscillator strengths are small for the HOMO-LUMO transitions. In Fig. 4, the absorption onsets in the imaginary part of the NC dielectric function ϵ_{NC} show that the strongest optical transitions correspond to higher energies than the gap energy. The dielectric functions ϵ_{SC} of the supercell have been calculated within the independent-particle approximation[17] using the DFT-LDA electronic structures, whereas the spectra for the NCs (Im ϵ_{NC}) are obtained by means of $\epsilon_{SC}=f\epsilon_{NC}+(1-f)$, where f is the crystallite-supercell volume ratio. This procedure allows one to compare better the intensities of the peaks in the spectra of different NC's. The energy distribution of the oscillator strengths for the NC's with $\{Si_{17}\}$ cores show that the indirect-gap character of Si bulk is still present, independently of passivation and level of oxidation. The onset of absorption for NC's reflects the trends for the pair excitation energies and gaps presented in Table I.

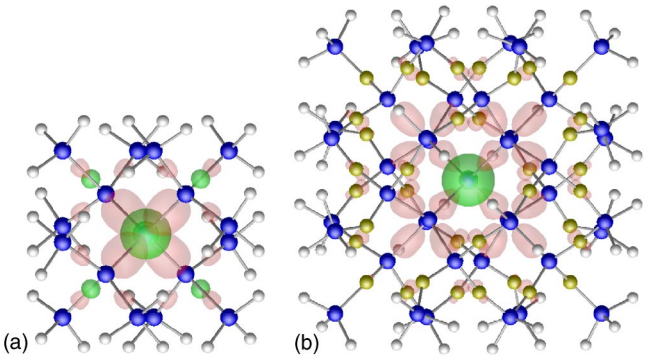

FIG. 3. (Color online) Square of the wave functions for the HOMO (dark) and LUMO (light) states in the nanocrystallites $\{Si_{17}\}$-H_{36} (a) and $\{Si_{17}\}$-$O_{36}Si_{24}H_{60}$ (b). The Si (the largest spheres), O (intermediate size spheres), and H (the smallest spheres) atoms are indicated. The isosurfaces correspond to values close to the maximum values.

In order to verify the role played by oxygen-related defects at the NC/oxide interface or surface of the NC, we study a Si double-bonded to an O atom. We replace a two-hydrogen termination by one oxygen atom in the oxidized NC $\{Si_{41}\}$-$O_{60}Si_{42}H_{108}$. The resulting HOMO-LUMO gap is only 20 meV lower than for the fully oxidized NC, showing that a defect of the type Si=O is less important for determining the gap, as depicted from previous calculations.[12–15] Analogously, if a single oxygen is removed from a Si-O-Si bond in the same fully oxidized NC, the change in the HOMO-LUMO gap is also few meV. Both results suggest a limited influence of oxygen related defects and type of oxygen bonds (single or double) on the HOMO-LUMO gap of NC's, at least when a complete backbond oxidation already occurred. Taking into account only Si, O, and H species, the observed redshift of the PL peak position of about 1 eV could be better explained by the passivation with OH without the consideration of oxygen-related defects.[4]

In conclusion, we have studied the effect of backbond oxidation on Si NC's in comparison to NC's passivated with

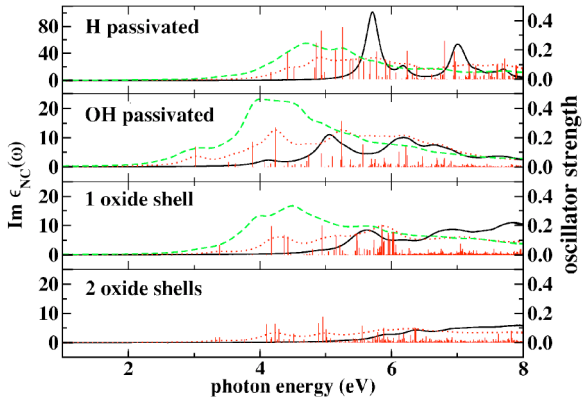

FIG. 4. (Color online) Imaginary part of the dielectric function versus photon energy of Si NC's with different core sizes. Solid lines: $\{Si_5\}$ core, dotted lines: $\{Si_{17}\}$ core, and dashed lines: $\{Si_{41}\}$ core. The vertical lines represent the oscillator strengths for the NC's with $\{Si_{17}\}$ core.

H atoms and OH group. Our first-principles calculations show the importance of the quantum confinement effects for both oxidized, OH- and H-passivated Si NC's. The blueshift measured in NCs after oxidation is related to the reduction of the core caused by the backbond oxidation. Conversely, the strong redshift measured in some NC's exposed to air is better explained by incorporation of oxygen via passivation with groups OH. Although the passivation with OH does not influence significantly the size of the Si core of the NC, the electronic properties and consequently the HOMO-LUMO gap are sensibly affected. No oxygen-related defects are needed to explain the gap shrinkage in NC's. The latter mainly occurs due to the weaker localization of the LUMO state of NC's caused by the presence of oxygen atoms in the outermost shells.

Financial support from the European Community within the RTN NANOPHASE (Contract No. HPRN-CT-2000-00167) and Deutsche Forschungsgemeinschaft (Project No. Re 1346/12-1) is acknowledged. The calculations were partly performed at the Von Neumann Institut for Computing (NIC) in Jülich, Germany as a part of the Project No. HJN21/2003. We would like to thank H.-Ch. Weißker for discussions and suggestions.

[1] K. D. Hirschman, L. Tsybekov, S. P. Duttagupta, and P .M. Fauchet, Nature (London) **384**, 338 (1996).
[2] A. Fowler, Phys. Today **50**, 50 (1997).
[3] L. T. Canham, Appl. Phys. Lett. **57**, 1046 (1990).
[4] M. V. Wolkin, J. Jorne, P. M. Fauchet, G. Allan, and C. Delerue, Phys. Rev. Lett. **82**, 197 (1999).
[5] J. P. Wilcoxon, G. A. Samara, and P. N. Provencio, Phys. Rev. B **60**, 2704 (1999).
[6] G. Ledoux, O. Guillois, D. Porterat, C. Reynaud, F. Huisken, B. Kohn, and V. Paillard, Phys. Rev. B **62**, 15 942 (2000).
[7] I. Vasiliev, S. Öğüt, and J. R. Chelikowsky, Phys. Rev. Lett. **86**, 1813 (2001).
[8] Z. Zhou, L. Brus, and R. Friesner, Nano Lett. **3**, 163 (2003).
[9] M. L. Brongersma, A. Polman, K. S. Min, E. Boer, T. Tambo, and H. A. Atwater, Appl. Phys. Lett. **72**, 2577 (1998).
[10] M. Zacharias, J. Heitmann, R. Scholz, U. Kahler, M. Schmidt, and J. Bläsing, Appl. Phys. Lett. **80**, 681 (2002).
[11] A. A. Seraphin, E. Werwa, and K. D. Kolenbrander, J. Mater. Res. **12**, 3386 (1997).
[12] I. Vasiliev, J. R. Chelikowsky, and R. M. Martin, Phys. Rev. B **65**, 121302 (2002).
[13] A. B. Filonov, S. Ossicini, F. Bassani, and F. Arnaud d'Avitaya, Phys. Rev. B **65**, 195317 (2002).
[14] M. Luppi and S. Ossicini, J. Appl. Phys. **94**, 2130 (2003).
[15] A. Puzder, A. J. Williamson, J. C. Grossman, and G. Galli, Phys. Rev. Lett. **88**, 097401 (2002).
[16] G. Kresse and J. Furthmüller, Comput. Mater. Sci. **6**, 15 (1996); Phys. Rev. B **54**, 11 169 (1996).
[17] B. Adolph, J. Furthmüller, and F. Bechstedt, Phys. Rev. B **63**, 125108 (2001).
[18] H.-Ch. Weissker, J. Furthmüller, and F. Bechstedt, Phys. Rev. Lett. **90**, 085501 (2003).
[19] K. C. Scheer, R. A. Rao, R. Muralidhar, S. Bagchi, J. Conner, L. Lozano, C. Perez, M. Sadd, and B. E. White, Jr., J. Appl. Phys. **93**, 5637 (2003).
[20] Y. Yasuda, H. Ikeda, and S. Zaima, Appl. Surf. Sci. **113-114**, 579 (1997).
[21] S. N. Kuznetsov, A. A. Saren, V. B. Pikulev, Y. E. Gardin, and V. A. Gurtov, Appl. Surf. Sci. **191**, 247 (2002).
[22] H.-Ch. Weissker, J. Furthmüller, and F. Bechstedt, Phys. Rev. B **67**, 245304 (2003).
[23] H. Hofmeister and P. Ködderitzsch, Nanostruct. Mater. **12**, 203 (1999).
[24] H. Hofmeister, F. Huisken, and B. Kohn, Eur. Phys. J.: Appl. Phys. **9**, 137 (1999).
[25] J. D. Torre, J.-L. Bocquet, Y. Limoge, J.-P. Crocombette, E. Adam, G. Martin, T. Baron, P. Rivallin, and P. Mur, J. Appl. Phys. **92**, 1084 (2002).